

Ultramafic Lower Mantle Inclusions in the Capii-6 Lonsdaleite Diamond: Implications for Earth's Deep Interior

Inclusiones Ultramáficas del Manto Inferior en el Diamante Lonsdaleítico Capii-6: Implicaciones para el Interior Profundo de la Tierra

Jaime L. B. Presser*, [♠]

*JP Exploration, Asunción, Paraguay. Email: presserjaime@gmail.com.

Abstract.- This study presents a detailed analysis of the lonsdaleite diamond Capii-6, an exceptional specimen originating from the Earth's lower mantle. The presence of lonsdaleite in this diamond was confirmed through Raman spectroscopy and X-ray diffraction (XRD), techniques that also allowed the identification of characteristic lower mantle mineral inclusions, such as breyite (formerly Ca-perovskite), bridgmanite (or its retrogressed product, enstatite/corundum), and ferropericlase = Ultramafic Association. The "diamond's" lithostatic formation pressure was constrained to 25–29 GPa using ferropericlase geobarometry and the pressure-dependent FWHM of the Raman D-peak, consistent with derivation from the lower mantle. However, localized pressure peaks of 45-56 GPa, recorded, indicate transient overpressures far exceeding lithostatic conditions. These transient overpressures could be attributed to localized stress amplification during slab deformation, possibly related to a significant rupture of the subducting slab in the lower mantle. Raman spectroscopic analysis revealed three main spectral types within the diamond, suggesting that it is not a defect-free natural cubic diamond. Additionally, an inverse relationship was observed between the intensity of the D-peak and the FWHM values, a behavior that contrasts with typical natural diamonds. X-ray diffraction patterns showed a prominent peak near 75.6° 20 (a 220 reflection from diamond, overlapping with that of lonsdaleite), a less intense peak around 43.72° 20, and a characteristic triplet peak for lonsdaleite. Machine Learning analysis indicated a predominant composition of lonsdaleite, accounting for 94.6%, characterized by nanocrystals with a size of 12 ± 1 nm. The remaining percentage corresponds to cubic IIa diamond, with a crystal size of 50 ± 5 nm. These findings significantly contribute to the understanding of ultradeep diamond formation and the dynamic processes within the Earth's mantle, potentially linking them to Nazca plate subduction; consequently, the mineral inclusion is interpreted as a xenolith from a subducted slab within the lower mantle.

Keywords: lonsdaleite diamond, lower mantle, Raman spectroscopy, X-ray diffraction, mineral inclusions, high pressure, Nazca plate, lonsdaleite, Ca-perovskite, enstatite, ferropericlase.

Resumen.- Este estudio presenta un análisis detallado del diamante lonsdaleítico Capii-6, un espécimen excepcional originado en el manto inferior de la Tierra. La presencia de lonsdaleíta en este diamante fue confirmada mediante espectroscopía Raman y difracción de rayos X (XRD), técnicas que también permitieron identificar inclusiones minerales características del manto inferior, como breyita (anteriormente Ca-perovskita), bridgmanita (o su producto de retrogresión, enstatita/corindón) y ferropericlasa = Asociación Ultramáfica. La presión de formación litostática del "diamante" se estimó entre 25-29 GPa mediante geobarometría de ferropericlasa y la relación entre el FWHM del pico D en espectros Raman y la presión, consistente con un origen en el manto inferior. Sin embargo, picos de presión localizados de 45-56 GPa, registrados, indican sobrepresiones transitorias que exceden ampliamente las condiciones litostáticas. Estas sobrepresiones transitorias podrían atribuirse a la amplificación localizada de la tensión durante la deformación de la placa en subducción, posiblemente relacionada con una ruptura significativa de la placa subductada en el manto inferior. El análisis espectroscópico Raman reveló tres tipos espectrales principales dentro del diamante, lo que sugiere que no se trata de un diamante cúbico natural libre de defectos. Además, se observó una relación inversa entre la intensidad del pico D y los valores de FWHM, un comportamiento que difiere de los diamantes naturales típicos. Los patrones de difracción de rayos X mostraron un pico prominente cerca de 75.6° 2θ (reflexión 220 del diamante, que se superpone con el de la lonsdaleíta), un pico menos intenso alrededor de 43.72° 20 y un pico tridente característico de la lonsdaleíta. El análisis mediante Machine Learning reveló una composición



predominante de lonsdaleíta, representando un 94.6%, caracterizada por nanocristales de un tamaño de 12 ± 1 nm. El porcentaje restante corresponde a diamante IIa cúbico, con un tamaño de cristal de 50 \pm 5 nm. Estos hallazgos contribuyen significativamente a la comprensión de la formación de diamantes ultraprofundos y los procesos dinámicos dentro del manto terrestre, posiblemente vinculándolos a la subducción de la placa de Nazca; consecuentemente, la inclusión mineral se interpreta como un xenolito de la placa de Nazca subductada en el manto inferior.

Palabras clave: diamante lonsdaleítico, manto inferior, espectroscopía Raman, difracción de rayos X, inclusiones minerales, alta presión, placa de Nazca, lonsdaleíta, Ca-perovskita, enstatita, ferropericlasa.

Discussing diamonds is a topic so broad that it could easily fill a book of more than 300 pages, or even more. However, as a summary, it can be said that diamonds are essentially composed of carbon and represent a fascinating object of study in the fields of mineralogy and geology. This is not only due to their exceptional hardness and optical properties but also to the diversity of their origins and the variations in their structure and composition. Their formation occurs under extreme conditions of pressure and temperature, leading to the great variety of types found in nature, as mentioned by Litvin (2017), Orcutt et al. (2020), Afanasiev et al. (2000), Erlich and Hausel (2002), Tapper & Tapper (2011), Presser (2024), among others.

Types of Diamonds According to Their Origin and Formation

Lithospheric Mantle Diamonds: These are the most common and form at depths between 100 and 300 km in the Earth's mantle (Litvin, 2017; Erlich and Hausel, 2002; Tapper & Tapper, 2011; Sorokhtin, 2016; Stachell *et al.*, 2022; Harris *et al.*, 2022; Smith *et al.*, 2022). They are commonly found in kimberlitic rocks and are classified into two main types:

Peridotitic: They contain silicate inclusions such as olivine, diopside, Mg-chromite, and Crgarnets, and exhibit a carbon isotopic composition similar to that of the mantle.

Eclogitic: They contain inclusions of minerals such as Cr-free garnet and omphacitic pyroxene, with greater variability in their carbon isotopic composition.

Sublithospheric (Ultra-Deep) Diamonds: These form at greater depths, even in the lower

mantle, exceeding 750 km in depth. These diamonds may contain inclusions of minerals such as majorite garnet, ringwoodite, breyite, larnite, jeffbenite, bridgmanite, ferropericlase, and stishovite, as well as carbonates such as aragonite, dolomite, nyerereite, nahcolite, among others (Kaminsky, 2012; Walter *et al.*, 2022; Smith *et al.*, 2022; Presser, 2024).

Impact Diamonds: Generated by meteorite or asteroid impact events. They are found in:

Meteorites: With a microcrystalline structure (Németh *et al.*, 2022; Németh *et al.*, 2023; Presser *et al.*, 2020; Presser & Sikder, 2024).

Astroblemes: Impact structures, such as the Popigai crater, where impact diamonds often contain lonsdaleite, a hexagonal polymorph of carbon (*cf.*, Masaitis, 2019 and references in the text; Presser *et al.*, 2017; Presser *et al.*, 2024c).

Lonsdaleite Diamonds: Diamonds with a cubic (mostly) and hexagonal structure instead of the typical cubic structure. They have been found both in impact craters and in the lower mantle, suggesting different formation mechanisms than lithospheric diamonds (Presser *et al.*, 2024a; 2024b; Presser, 2025; Presser *et al.*, 2020; Presser & Sikder, 2024; Presser *et al.*, 2024c).

Artificial Diamonds: Synthesized in the laboratory under controlled high-pressure and high-temperature conditions. They are mainly used in industrial applications due to their abrasive properties (see, for example, Sung, 2021).

Carbonado Diamond: Carbonado is a variety of polycrystalline diamond (Cartigny, 2010), generally black, brown, or dark gray in color, with a microcrystalline and porous structure (Afanasiev *et al.*, 2024). It is composed of sintered diamond grains and is distinguished

by its high resistance to abrasion (Afanasiev *et al.*, 2024), the presence of various mineral inclusions, as well as a specific carbon isotopic composition (Cartigny, 2010; Petrovsky *et al.*, 2010). Carbonados are mainly found in alluvial deposits in Brazil and Central Africa (Afanasiev *et al.*, 2024, Cartigny, 2010). Regarding their origin, the main hypotheses include:

Mantle Origin: It is proposed that carbonado formed from subducted organic carbon in the mantle (Cartigny, 2010), where it transformed into diamond under high-pressure and high-temperature conditions. The carbon and nitrogen isotopes of Dachine komatiite diamonds show similarities with carbonados, supporting this hypothesis (Cartigny, 2010).

Crustal Origin: Another hypothesis suggests that carbonado formed in uranium-rich crustal environments, where radiation induced diamond crystallization (Afanasiev *et al.*, 2024).

Origin from Shungite-Type Rocks: It is proposed that carbonados originated from subducted shungite-type rocks that later transformed into diamond (Afanasiev *et al.*, 2024).

Additionally, **carbon-saturated fluid**: It is also suggested that carbonados formed from a carbon-saturated fluid (Cartigny, 2010). It is important to note that: The mineral inclusions found in carbonado are secondary, formed after the creation of the diamond (Afanasiev *et al.*, 2024). Carbonados exhibit low nitrogen aggregation (Cartigny, 2010). The growth of carbonados could be related to a decrease in carbon saturation (Petrovsky *et al.*, 2010). It is worth noting that Haggerty (2017) provides an academic synthesis on the study of carbonado diamonds.

Classification of Diamonds According to Their Nitrogen Content

According to Tappert & Tappert (2011), Sorokhtin (2019), among others, diamonds are classified into two main types: Type I and Type II, based mainly on the presence and form of nitrogen within their crystal structure. This classification is crucial because it directly affects

their colors and other physical properties.

Type I: Type IaA: Most of the nitrogen is found in substitutional pairs in the crystal lattice. Type IaB: Nitrogen forms aggregates of four atoms around a vacancy. Type IaAB: Diamonds containing both types of nitrogen aggregates (IaA and IaB). Type Ib: Nitrogen is found as individual substitutional atoms in the crystal lattice. These diamonds are less common in nature and are more frequent in synthetic diamonds.

Type II: Type IIa: They have practically no nitrogen impurities and are usually colorless. They exhibit electrical conductivity and semiconductor behavior. Type IIb: They contain boron as an impurity, which gives them semiconductor properties and a bluish coloration.

Diamond Deposits

Diamonds are located in various types of geological deposits (Akulov, 2022; Erlich & Hausel, 2002):

Kimberlites: These are igneous rocks that transport diamonds from great depths, being the main sources of these minerals (Mitchell, 1986).

Lamproites: Other igneous rocks that can also contain diamonds (Mitchell & Bergman, 1991; Mitchell, 1995).

Alluvial Deposits (placers): Diamonds are transported and accumulated by water action in rivers and coastal areas, showing signs of mechanical wear (e.g., Sorokhtin, 2016).

Metamorphic Rocks: In rare cases, diamonds form in metamorphic rocks under extreme pressure conditions (*cf.* Dobrzhinetskaya *et al.*, 2012).

To maintain the brevity of these summarized lines, other types of diamond occurrences, such as those found in komatiites, lamprophyres, and ophiolites, etc. have been omitted.

Additional Morphological Characteristics

In addition to classifications based on origin and nitrogen content, the morphological characteristics of diamonds, such as crystal shape, surface texture, and the presence of inclusions and structural defects, are crucial for understanding their geological history. These characteristics may be related to the growth, dissolution, alteration, or transport phases of diamonds, and include aspects such as (Afanasiev *et al.* 2000; Tapper & Tapper, 2011):

Growth Forms: Octahedron, cube, rhombododecahedron, and tetragontrioctahedron.

Surface Morphology: Includes reliefs such as protrusions, grooves, trigonal and ditrigonal layers, pits, and pitting.

Textures: Smooth, rough, laminated surfaces, with dissolution patterns and mechanical wear effects.

Essentially, this work compiles existing information from Raman and XRD spectra (Presser, 2024a and references), which were edited, reinterpreted, and finally fitted with the aid of Machine Learning AI (see appendix).

This work aims to present an illustrated synthesis of the lonsdaleite diamond Capii-6, one of the diamonds originally studied by Presser & Sikder (2022) through extensive Raman spectral mapping. Subsequently, this diamond was the subject of detailed X-ray diffraction (XRD) studies (Presser et al., 2024a and Presser et al., 2024b), which revealed its particular content of lonsdaleite and lower mantle mineral inclusions (Presser, 2024a; Presser 2024b; Presser, 2025; Presser et al., 2024a; 2024b). Thus, it is believed that the Capii-6 diamond would be the first fully documented evidence of a lonsdaleite diamond, which, as will be seen later, would also be the first documented evidence of a lonsdaleite diamond with a lower mantle ultramafic association mineral inclusion.

Background on Diamonds in Capilbary

The chronological background of Capiibary diamonds is briefly summarized as follows:

1825: The first report of diamonds in Paraguay is recorded, specifically in Santa María, Misiones Department (Eastern Paraguay) (*cf.*, Presser, 2019).

1960s: Artisanal diamond mining would

have begun in the city of Capiibary, San Pedro Department (Eastern Paraguay). A team of gold prospecting geologists, in collaboration with local resident Modesto Quiñonez, identifies diamond indicator minerals (LIM/KIM/DIM) in the bed of the Retama stream. This finding marks the beginning of diamond exploration in the region (see comments in Presser, 2024a).

2001: Presser presents the Curuguaty Project, a formal request for diamond prospecting and exploration in Canindeyú Department. This project is based on the theory that primary diamond sources, such as kimberlites, are found in cratonic areas with Archean basement. Sampling is conducted in a stream near a potential "kimberlite" intrusion, and a "kimberlitic mineral suite" including diamonds is found, thus confirming the presence of diamonds in the area and the potential of the Curuguaty Project (in the vicinity of the Capiibary region). This work publishes the first photograph of a Capiibary diamond (Fig. 1). (Presser, 2001).

2012: Smith, Bulanova, and Presser conduct the first scientific study of Capiibary diamonds. The external morphology, internal structure, mineral inclusions, nitrogen content, and aggregation state of the diamonds are analyzed.

2014: A more extensive study on Capiibary diamonds is published by Presser, Bulanova, and Smith. This work, based on the analysis of approximately a dozen and a half diamonds, describes their characteristics, including the presence of highly forsteritic olivine inclusions

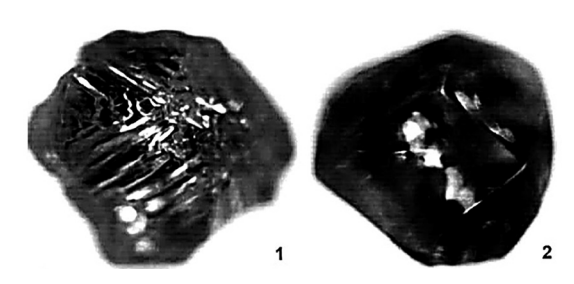


Figure 1. First published photographs of Capiibary diamonds (Presser, 2001). A macroscopic colorless diamond of approximately 1 mm is observed, with pseudo-hemimorphic shapes (Front and back of).

(Fo_{_92-94}) suggesting an origin in an Archean lithospheric mantle.

2016 - 2019: Presser continues to investigate diamond occurrences in Paraguay and publishes various works on the subject, including information on Capiibary diamonds (see references in Presser, 2024).

2022: Presser & Sikder publish a Raman spectroscopic analysis of Capiibary diamonds and their mineral inclusions. It is discovered that most of the studied diamonds exhibit characteristics of lonsdaleite diamonds, a hexagonal polymorph of carbon that forms under extreme pressures.

2024: Presser publishes the book "The Capiibary 'Diamonds': A window to the lower mantle," which compiles research on Capiibary diamonds, including Raman spectroscopic analyses, XRD analyses, and studies of mineral inclusions. The presence of lonsdaleite diamonds in Capiibary is confirmed, and it is proposed that their origin lies in the lower mantle, possibly from the subducted Nazca plate.

2024: A study by Jaime L.B. Presser presents the discovery of unusual diamonds in the Capiibary region, Paraguay. These diamonds contain a mixture of cubic diamond and lonsdaleite, a rare hexagonal polymorph of diamond. Their mineral composition suggests formation in the Earth's lower mantle under high pressures and temperatures. The origin is attributed to the subducted Nazca plate. The finding provides new information on diamond formation and processes in the deep interior of the Earth.

2024: A study by Jaime L.B. Presser reviews the concept of lonsdaleite, a nanocomposite of diamond with disordered cubic and hexagonal layers. Detection methods, such as Raman spectroscopy and X-ray diffraction (XRD), are described to identify lonsdaleite in the Earth's mantle. A linear relationship between formation pressure and the full width at half maximum (FWHM) of the D-peak in Raman spectra is established, culminating in an equation to estimate the formation depth of diamonds. Finally, it is concluded that lonsdaleite is not a simple





Figure 2. General appearance of the Capii-06 diamond under natural light (top) and in an SEM image. The figures show the slightly distorted rhombohedral shape of an intact crystal.

hexagonal polytype but a complex material. Raman and XRD spectra of one of the lonsdaleite diamonds from Capiibary (Capii-06) are used as an example of what is presented in the text.

This chronological journey illustrates how interest in Capiibary diamonds has grown over the decades, driven by scientific research that has revealed the uniqueness of these gems and their potential to understand geological processes in the Earth's mantle.

General Characteristics

The Capii-06 diamond is a macroscopic crystal (~2 mm) with a series of unique characteristics (Figs. 2a-2b):

Color: Colorless with a slight smoky tone. Shape: Slightly distorted rhombohedron (elongated).

Integrity: Mostly intact.

Inclusions: Contains mostly black, micrometer-sized mineral inclusions.

Birefringence: Exhibits anomalous birefringence.

Raman Spectroscopy Analysis

Raman spectroscopy studies on Capii-06 revealed three main spectral types:

Type I: Characterized by a strong D-peak

(diamond) around 1331 cm⁻¹ with a narrow FWHM (~ 5 cm⁻¹), indicating high crystallinity similar to lithospheric diamonds. No significant G-peak (graphite) or peak near 1450 cm⁻¹ (d-peak or diaphite) is observed. This type is the most frequent, observed in 68% of the measured spectra. A subtype may exhibit weak peaks in the d and G regions within similar characteristics (Presser *et al.*, 2024b). (Figs. 3a-3b).

Type II: Moderate-intensity D-peak around 1331 cm⁻¹ accompanied by a prominent G-peak

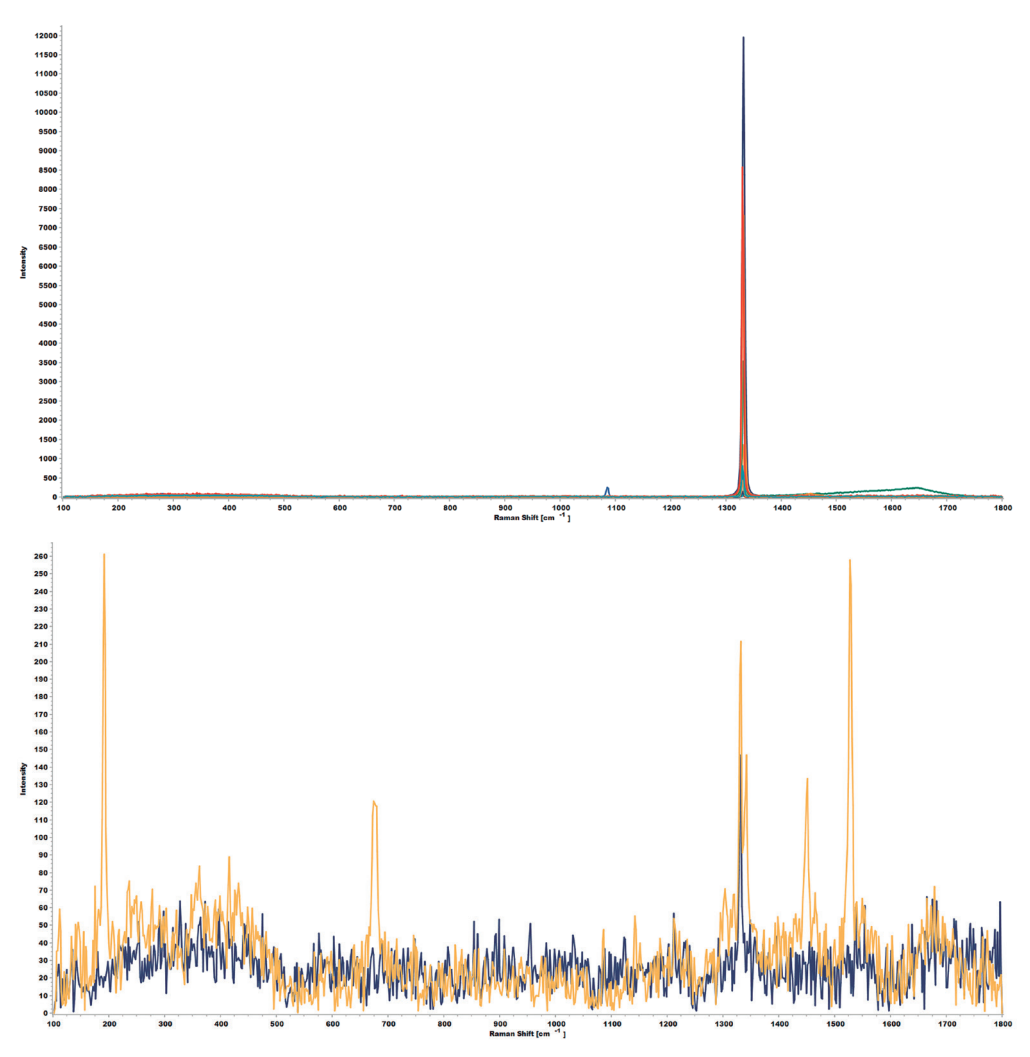


Figure 3a. Raman spectra of Type I. **a)** Raman spectrum of **Type I**: Characterized by a strong D-peak (diamond) around 1331 cm⁻¹ with a narrow FWHM (< 5 cm⁻¹), indicating high crystallinity similar to lithospheric diamonds. No significant G-peak (graphite) or peak near 1450 cm⁻¹ (d-peak or diaphite) is observed. This type is the most frequent, observed in 68% of the measured spectra. **3b)** This spectrum is a subtype of Type I shown and commented on in Figure 3a. This subtype may exhibit weak peaks in the d and G regions, maintaining similar characteristics.

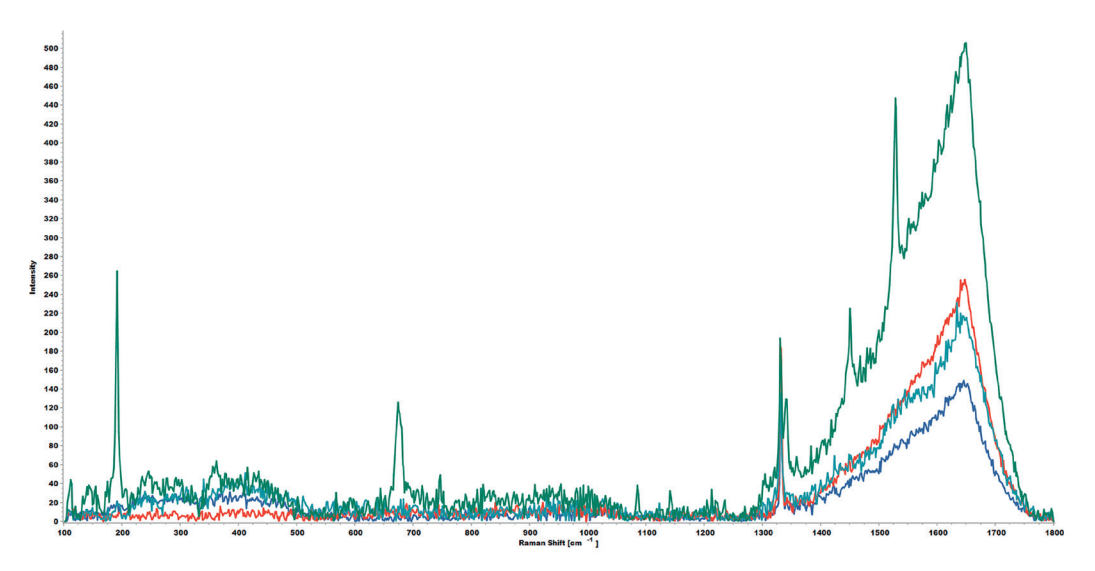


Figure 4. Raman spectrum of Type II: Moderate-intensity D-peak around 1331 cm⁻¹ accompanied by a prominent G-peak (normal or upshifted wavenumber), with or without a distinct d-peak. The FWHM varies from low to high.

(normal or upshifted wavenumber), with or without a distinct D-peak. The FWHM varies from low to high (Presser *et al.*, 2024b). (Fig. 4).

Type III: Pronounced D-peak around 1330 cm⁻¹ and G-peak (normal or upshifted wavenumber), with M-shaped profiles. The D-peak is slightly shifted to higher wavenumbers compared to typical diamond. The FWHM is very

high (Presser et al., 2024b). (Fig. 5).

The presence of multiple spectral types within Capii-06 suggests that it is not a defect-free natural cubic diamond. (Presser, 2024a, b; Presser *et al.*, 2024a, 2024b) Additionally, the relationship between the intensity of the D-peak and the FWHM values indicates an inverse correlation, a behavior different from typical natural

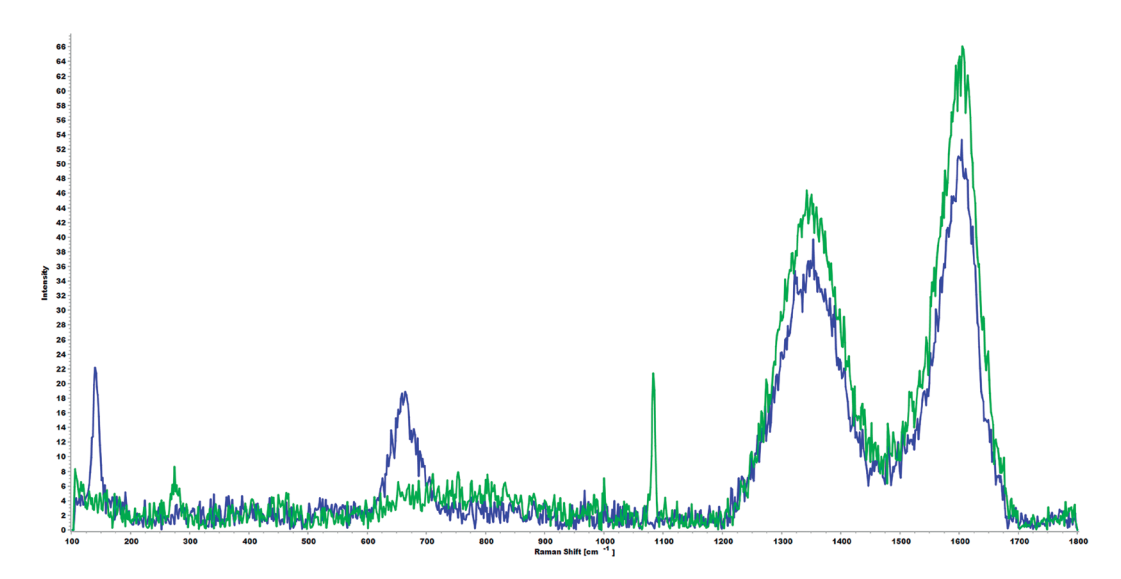


Figure 5. Raman spectrum of Type III: Pronounced D-peak around 1330 cm⁻¹ and G-peak (normal or upshifted wavenumber), with M-shaped profiles. The D-peak is slightly shifted to higher wavenumbers compared to typical diamond. The FWHM is very high.

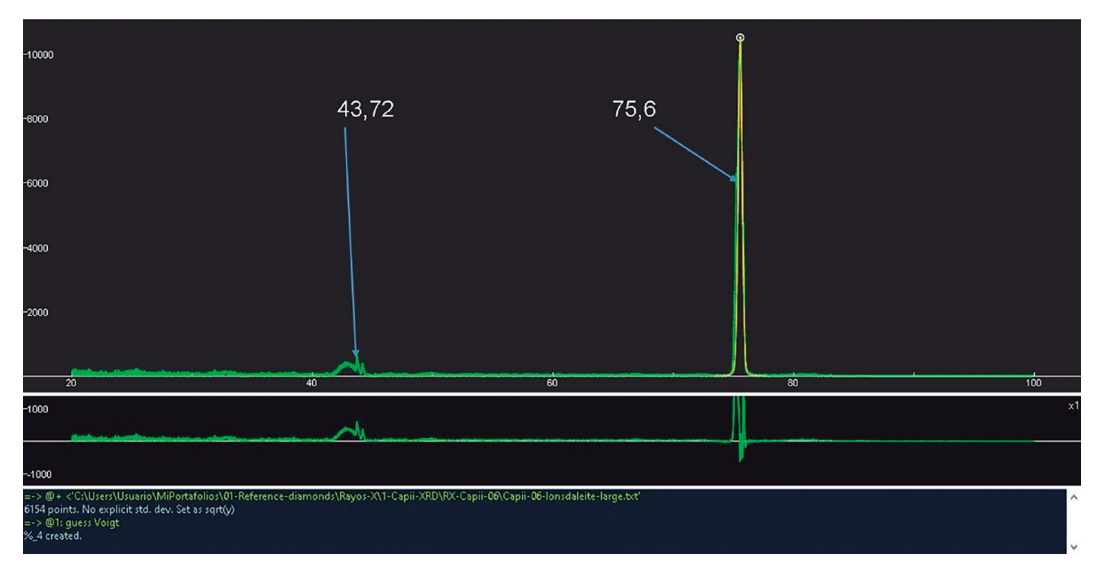


Figure 6. XRD spectrum of a lower mantle lonsdaleite diamond. A prominent peak is observed at 75° (110-220) and another less intense peak at 43.72° (111) 2θ degrees. The peak at 75° may be more intense due to overlap with cubic diamond. Lonsdaleite diamond Capii-6 (figure as in Presser, 2025).

diamonds. (Presser, 2024)

X-ray Diffraction (XRD) Analysis

XRD analysis of Capii-06 also confirms the presence of lonsdaleite. The diffraction pattern shows:

A prominent peak (diamond/lonsdaleite) near the 75.6° 2θ peak (220 reflection of dia-

mond) [Presser, 2025; Presser *et al.*, 2024a, b]. (Fig. 6).

A less intense peak around 43.72° 2θ (111 reflection of diamond), which appears as a "hill-shaped peak" between 40° and 50° 2θ [Presser, 2025; Presser *et al.*, 2024a, b]. (Fig. 7).

The characteristic "triplet peak" between 43° and 44° 2θ, a diagnostic signature of lonsdaleite

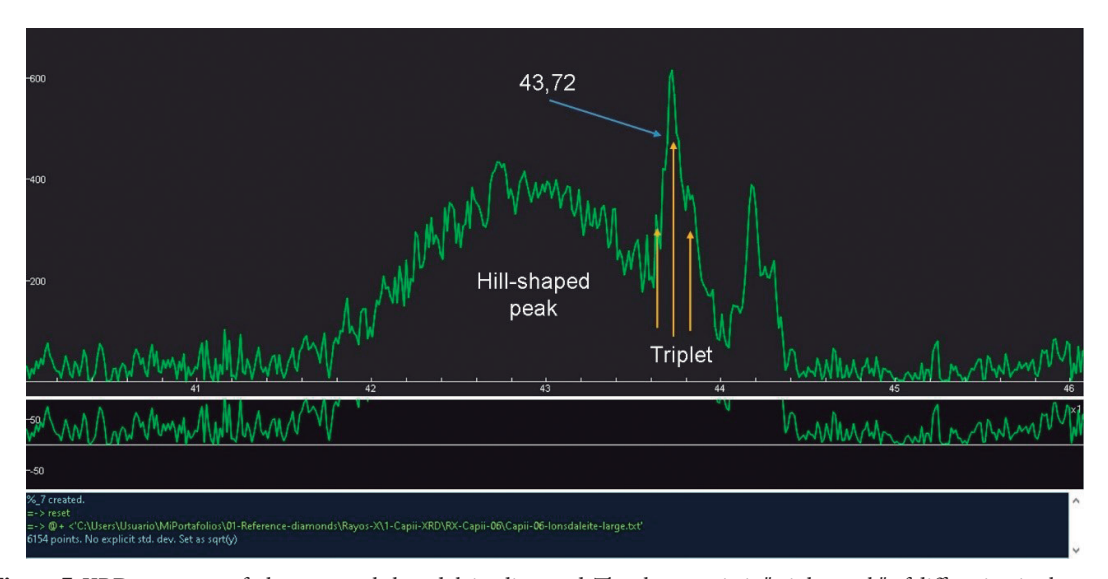
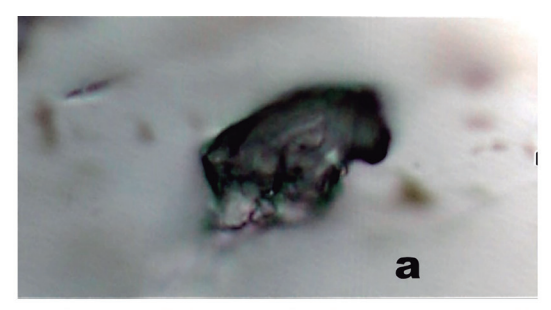


Figure 7. XRD spectrum of a lower mantle lonsdaleite diamond. The characteristic "triplet peak" of diffraction is observed between 40° and 50° (100-111-101), along with the peak at 43.72° (=111) 2θ degrees. Capii-6 (figure as in Presser, 2025).





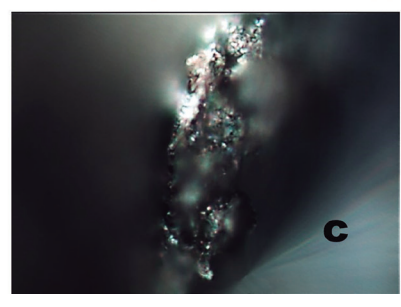


Figure 8. Microphotographs of well-identified mineral inclusions in the Capii-06 diamond: a) Bridgmanite (ashy tone and marked relief), b) Ferropericlase (iridescent), c) Calcite with irregular shape and irregular birefringence. These inclusions were previously highlighted in Presser & Sikder (2022).

(Presser, 2025).

Mineral Inclusions

Both Raman spectroscopy and XRD analysis revealed a series of mineral inclusions in Capii-06:

Identified by Raman Spectroscopy

Breyite (retrogressed products of Ca-perovskite=cPv) [Presser & Sikder, 2024; Presser *et al.*, 2024b]. (Fig. 9).

Enstatite and corundum (retrogressed products of bridgmanite) [Presser & Sikder, 2024; Presser *et al.*, 2024b]. (Figs. 8a and 9).

Ferropericlase or magnesiowüstite (Presser & Sikder, 2024; Presser *et al.*, 2024b) [Figs 8b

and 9].

Sulfides (chalcopyrite, pentlandite, and tausonite) [Presser & Sikder, 2024; Presser *et al.*, 2024b]. (Fig. 10).

Identified by XRD

Bridgmanite (Presser 2025; Presser *et al.*, 2024b) [Fig. 11].

Enstatite and corundum (as retrogressed products of bridgmanite) (Presser *et al.*, 2024b)

Breyite (as a retrogressed product of cPv) (Presser *et al.*, 2024b)

Ferropericlase (Presser & Sikder, 2024; Presser *et al.*, 2024b; Presser, 2025)

Calcite (low resolution) (Presser & Sikder, 2024; Presser *et al.*, 2024b).

The presence of these inclusions, particularly the bridgmanite-ferropericlase-cPv association, suggests that Capii-06 formed in the lower mantle (Presser, 2025; Presser *et al.*, 2024b); and these minerals reproduce an Ultramafic Association (cf. Walter *et al.*, 2022; Kaminsky, 2016 and also Litvin, 2017).

Formation Pressure

The formation pressure of ferropericlase in Capii-06 is estimated between 25 and 28 GPa (Presser etal., 2024b), based on the alignment of diffraction peaks with those of ferropericlase at different pressures. Additionally, using the relationship P (GPa) = $(0.3416 \times \text{FWHM}) + 3.2044$ (Presser, 2025) [Fig. 12 and Table 1], pressures ranging from 7 to 29 GPa were calculated for most of the analyzed spectra, with an additional group suggesting extreme pressures of up to 56 GPa. However, this latter group is evidence supporting such extreme conditions. These results reinforce the hypothesis that the Capii-06 diamond formed in the lower mantle, under high-pressure and high-temperature conditions.

Analysis and Discussion

The study of the lonsdaleite diamond Capii-6 highlights the complexity of diamond formation processes and the extreme conditions present

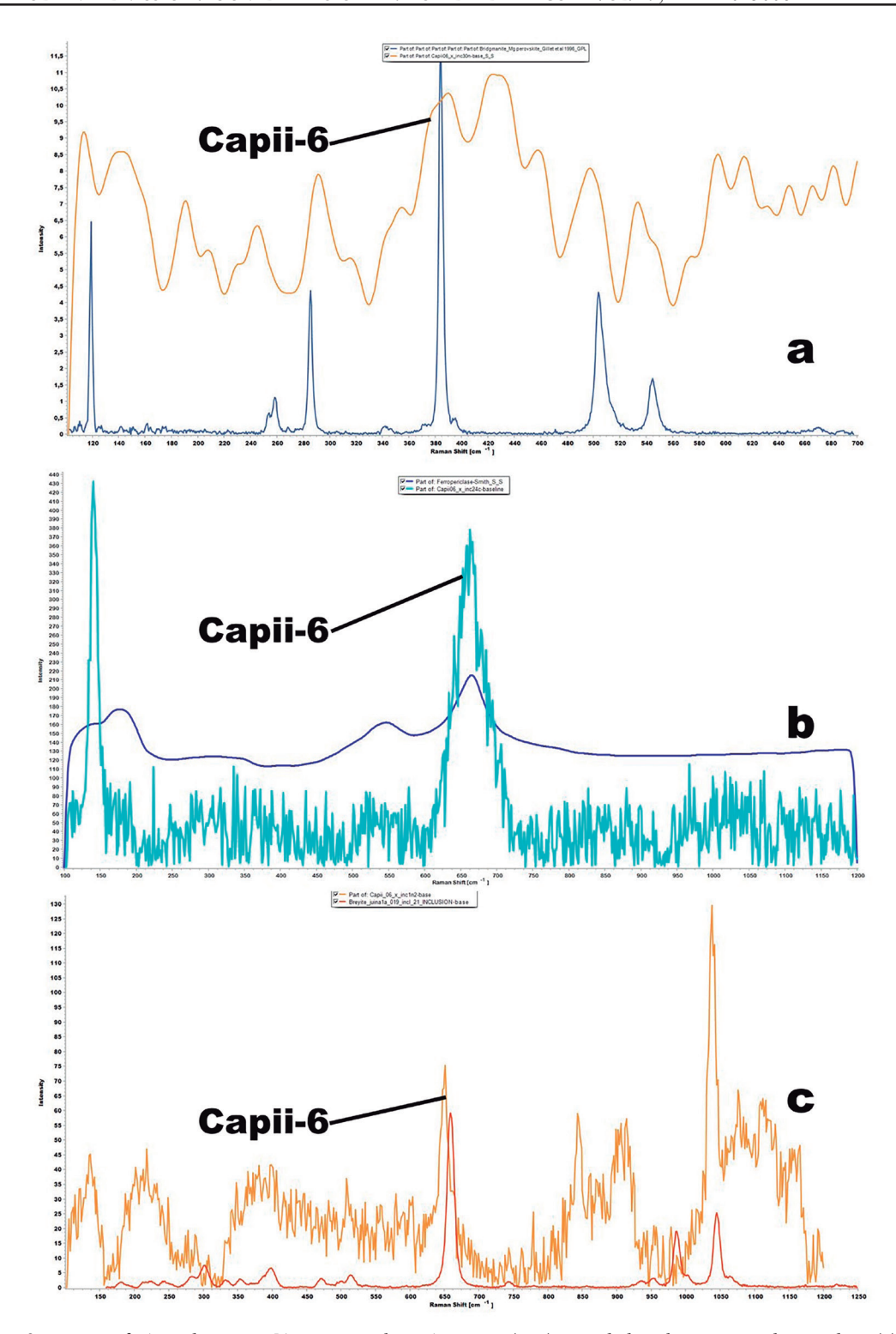


Figure 9. Spectra of: **a)** Bridgmanite. **b)** Ferropericlase. **c)** Breyite (cPv) recorded in the Capii-06 diamond. In (a), the raw spectrum was smoothed to reduce background noise, while in (b) and (c), the raw spectrum is shown. They are compared with reference spectra from Smith (2021) and Smith et al. (2022).

in the Earth's mantle. Diamonds, composed mainly of carbon, are fundamental objects of study in the fields of mineralogy and geology due to their unique properties and the diversity of their origins (Litvin, 2017; Orcutt *et al.*, 2020; Afanasiev *et al.*, 2000; Erlich & Hausel, 2012; Tapper & Tapper, 2011; Presser, 2024a). According to their origin, diamonds are classified into several categories:

1. Lithospheric Mantle Diamonds: They form at depths between 100 and 300 km (Litvin,

2017; Erlich & Hausel; Tapper & Tapper, 2011; Sorokhtin, 2016; Stachell *et al.*, 2022; Harris *et al.*, 2022; Smith *et al.*, 2022).

- **2.** Sublithospheric or Ultra-Deep Diamonds: They originate at greater depths of up to 1000 km, in the lower mantle (Kaminsky, 2012; Walter *et al.*, 2022; Smith *et al.*, 2022; Presser, 2024a).
- **3. Impact Diamonds:** Generated by meteorite or asteroid impact events (Németh *et al.*, 2022; Németh *et al.*, 2023; Presser & Sikder,

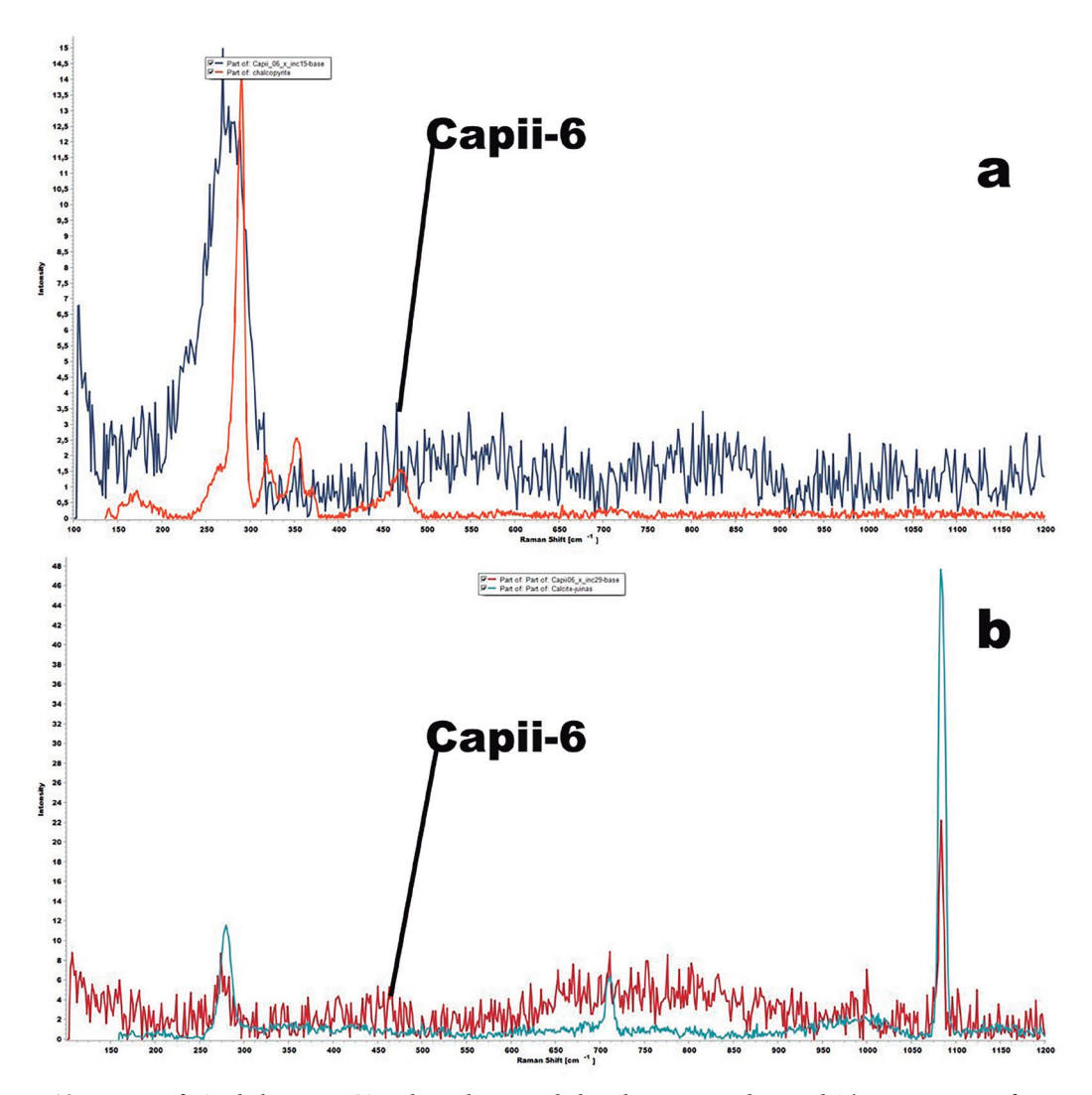


Figure 10. Spectra of: **a)** Chalcopyrite. **b)** Calcite also recorded in the Capii-06 diamond. The raw spectra of Capii-06 are compared with spectra from Smith's database (2021). In (a), slight interference from another sulfide's spectrum is observed (see Presser & Sikder, 2022).

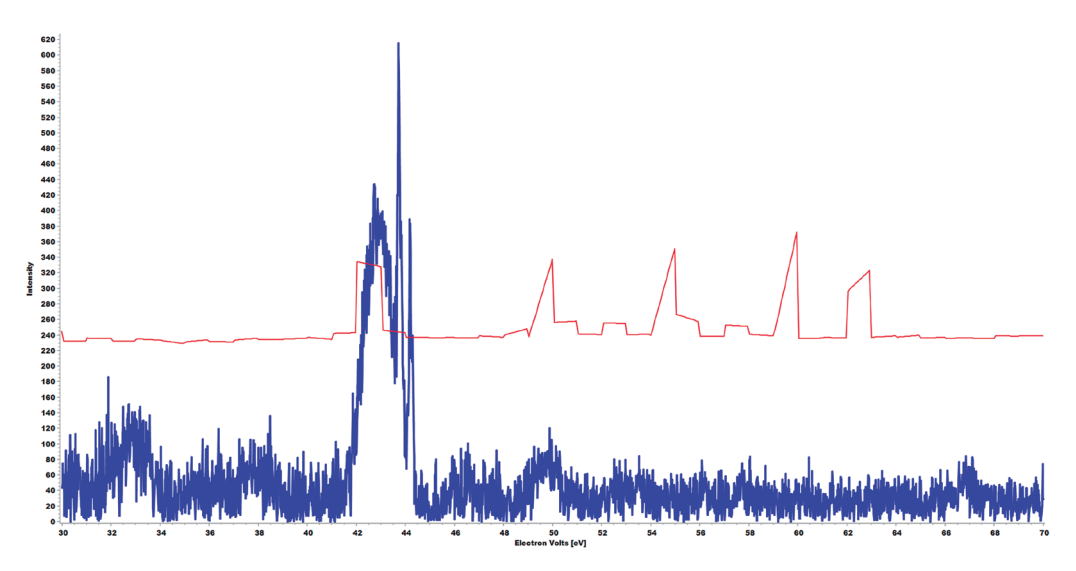


Figure 11. XRD spectrum of scanned bridgmanite (low resolution) from Guo et al., 2024 (top) versus XRD of Capii-6 (bottom). The correspondence between the most prominent peaks is noted.

2024).

4. Lonsdaleite Diamonds: They exhibit a cubic and hexagonal structure, instead of the typical cubic structure, and have been found both in impact craters (Masaitis, 2019) and in the lower mantle (Presser, 2025; Presser, 2024a, b).

The Capii-06 diamond belongs to this last category, suggesting an origin in the lower mantle (Presser, 2024a, b; 2025; Presser *et al.*, 2024a, b).

Additionally, the classification of diamonds according to nitrogen impurities (Types I and II) is fundamental for understanding their physical and spectroscopic properties. The work of Smith *et al.* (2012) and later of Presser *et al.* (2014) show that alluvial diamonds from Capiibary present Type I and Type II diamonds. Furthermore, the Machine Learning analysis applied to the Raman spectra and XRD data of this diamond estimates it to be a type IIa diamond

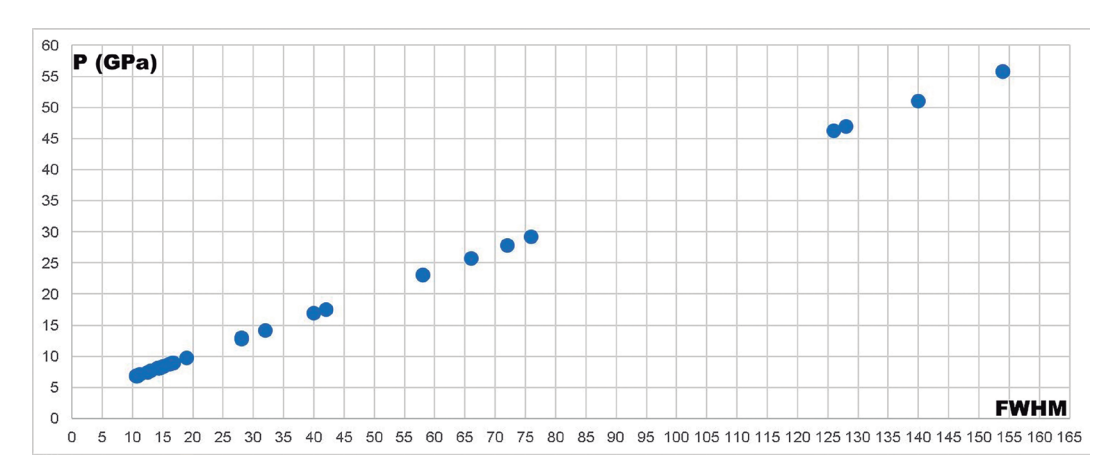


Figure 12. Selected Raman spectra from Table 1, showing pressure in GPa versus FWHM (Presser, 2025). The heterogeneity of the results is evident, with typical diamond pressures up to very high pressures, characteristic of lonsdaleite formation in the lower mantle (up to 29 GPa). The group of 4 measurements shows an extremely high value, which is commented on in the text. These four measurements are set aside in this work.

Table 1. Selected Raman spectra of the Capii-06 diamond. The D-peak (cm $^{-1}$), FWHM value (cm $^{-1}$), and calculated pressure (GPa) are indicated using the relationship P (GPa) = $(0.3416 \times \text{FWHM}) + 3.2044$.

ID	D-peak	FWHM	PGPa
Capii_06_x_inc2n	1345	28,0	13,0
Capii_06_x_inc3	1331	42,0	17,6
Capii_06_x_inc7	1332	16,8	8,9
Capii_06_x_inc1n2	1299	58,0	23,0
Capii_06_x_inc9	1332	14,4	8,1
Capii_06_x_inc10	1333	16,6	8,9
Capii_06_x_inc13	1332	32,0	14,1
Capii_06_x_inc14	1331	14,8	8,3
Capii_06_x_inc15b	1331	14,4	8,1
Capii_06_x_inc16b	1325	13,0	7,6
Capii_06_x_inc17	1330	76,0	29,2
Capii_06_x_inc18	1300	140,0	51,0
Capii_06_x_inc18a	1314	66,0	25,8
Capii_06_x_inc20	1331	14,2	8,1
Capii_VCU_06_01	1331	15,0	8,3
Capii_VCU_06_010	1331	14,4	8,1
Capii_VCU_06_012	1331	16,0	8,7
Capii_VCU_06_015	1330	14,4	8,1
Capii_VCU_06_015b	1330	14,4	8,1
Capii_VCU_06_015c	1330	10,6	6,8
Capii_VCU_x_06	1332	19,0	9,7
Capii06_x_inc2	1331	10,8	6,9
Capii06_x_inc2n	1345	28,0	12,8
Capii06_x_inc22	1334	11,2	7,0
Capii06_x_inc28	1330	10,8	6,9
Capii06_x_inc30n	1331	14,2	8,1
Capii06_x_inc31n	1330	10,6	6,8
Capii06_x_inc33n2	1330	58,0	23,0
Capii06_x_inc33n	1330	11,0	7,0
Capii06_x_inc34n	1336	15,2	8,4
Capii06_x_inc34n2	1334	72,0	27,8
Capii06_x_inc35n2	1354	154,0	55,8
Capii06_x_inc35n3	1334	40,0	16,9
Capii06_x_inc35n4	1334	12,5	7,5
Capii06_x_inc35n	1354	154,0	55,8
Capii06_x_inc24c	1349	126,0	46,2
Capii-6-29	1350	128,0	46,9
Capii06_VCU_06_03_Diamond	1332	16,4	8,8

(see Appendix).

Diamonds are mainly found in kimberlites (Mitchell, 1986), lamproites (Mitchell & Bergman, 1991; Mitchell, 1995), alluvial deposits (Sorokhtin, 2016), and, in rare cases, in metamorphic rocks (Dobrzhinetskaya *et al.*, 2012). In the case of Capiibary diamonds, they are associated with lamproites (Presser, 2024a; Presser & Sikder, 2022).

Morphological characteristics, such as crystal shape, surface texture, and the presence of inclusions, are key to reconstructing the geological history of diamonds (Afanasiev *et al.*, 2000; Tapper & Tapper, 2011). In the case of Capii-06, it is a slightly distorted rhombohedron, colorless with a smoky tone, containing micrometer-sized mineral inclusions.

Raman spectroscopy analyses performed on Capii-06 revealed three main spectral types, indicating a complex structure and not a defectfree natural cubic diamond (Presser, 2025):

Type I: Exhibits a strong D-peak around 1331 cm⁻¹, with a narrow FWHM (~ 5 cm⁻¹), indicating high crystallinity. No significant G-peak (graphite) or d-peak is observed. This type is the most frequent, representing 68% of the measured spectra (Presser, 2025).

Type II: Shows a moderate-intensity D-peak around 1331 cm⁻¹, accompanied by a prominent G-peak. The FWHM varies from low to high (Presser *et al.*, 2024b).

Type III: Characterized by a pronounced D-peak around 1330 cm⁻¹, slightly shifted to higher wavenumbers, and a G-peak with M-shaped profiles. The FWHM is very high (Presser, 2025).

The inverse correlation between the intensity of the D-peak and the FWHM is an anomalous behavior compared to typical natural diamonds, suggesting the presence of lonsdaleite and other unusual structural characteristics (Presser, 2025; Presser, 2024a).

X-ray diffraction (XRD) analysis confirmed the presence of (tenors of) lonsdaleite in Capii-06, showing characteristic peaks: a prominent peak near 75.6° 2θ, a less intense

peak around 43.72° 2 θ (with diffraction patterns shifted below 43.9° 2 θ , as observed in lonsdaleite diamonds according to Presser, 2025), and a triplet peak between 43° and 44° 2 θ (Presser, 2025; Presser *et al.*, 2024a, b). Which according to Machine Learning (Appendix) represents lonsdaleite 94.6%, characterized by nanocrystals with a size of 12 \pm 1 nm. The remaining percentage corresponds to cubic IIa diamond, with a crystal size of 50 \pm 5 nm.

Additionally, several mineral inclusions were identified in Capii-06, such as breyite (retrogressed products of Ca-perovskite), bridgmanite, enstatite/corundum (retrogressed products of bridgmanite), ferropericlase, sulfides, disordered graphite (Appendix) and calcite (Presser, 2024a; Presser & Sikder, 2024; Presser *et al.*, 2024a, b). The presence of the bridgmanite-ferropericlase-Ca-perovskite mineral association suggests that this diamond formed in the lower mantle (Presser, 2025; Presser *et al.*, 2024b), supporting its classification as an Ultramafic Association.

The formation pressure of ferropericlase was estimated between 25 and 28 GPa, which is consistent with lower mantle conditions (Presser, 2024a; Presser *et al.*, 2024b). Using the relationship between formation pressure and the FWHM of the D-peak in Raman spectra, pressures ranging from ~7 to 29 GPa were calculated for most of the analyzed spectra (Presser, 2025; Presser *et al.*, 2024b).

This "diamond" captures both lithostatic (~29 GPa) and ultrahigh (45–56 GPa) pressures, recorded by bridgmanite + ferropericlase. The 56 GPa peaks exceed lithostatic limits at the slab's depth, implying a dynamic origin. We propose that localized slab breakoff or shear rupture generated transient pressures, possibly via elastic rebound or adiabatic melting. This challenges the assumption that diamond inclusions solely reflect ambient lithostatic conditions.

Conclusions

The study of the Capii-6 diamond reveals that it formed under extreme conditions in the lower mantle, as confirmed by the presence of lonsdaleite molecules in the diamond crystal (lonsdaleite 94.6%, characterized by nanocrystals with a size of 12 ± 1 nm. The remaining percentage corresponds to cubic IIa diamond, with a crystal size of 50 ± 5 nm.), the characteristic mineral inclusions of this depth (such as bridgmanite, ferropericlase, and cPv = Ultramafic Association), and the estimated pressures between 25 to 29 GPa. The combination of analytical techniques, such as Raman spectroscopy, X-ray diffraction (XRD), and the study of mineral inclusions, provides crucial information for understanding the formation of ultra-deep diamonds and geodynamic processes in the Earth's interior.

So, this study demonstrates that diamonds can archive both lithostatic (~29 GPa) and ultrahigh (45–56 GPa) pressures within a single crystal. The 56 GPa peaks, recorded by bridgmanite + ferropericlase, defy lithostatic equilibrium and instead point to transient, event-driven overpressures. We propose that Nazca slab breakoff or shear rupture generated these extremes, underscoring diamonds' role as high-resolution monitors of deep-Earth dynamics. Our findings redefine inclusions not as static barometers but as witnesses to the mantle's most violent episodes.

Acknowledgements

I would like to express my sincere gratitude to Arif Sikder and Karl Mayer for their invaluable contribution through their previous publications. Their research and data have been fundamental to the completion of this review and have significantly enriched our understanding of the subject. Their prior work has laid the foundation for this study and has been a constant source of inspiration and guidance. I sincerely appreciate their generosity in sharing their knowledge and resources, which has allowed this research to be carried out successfully." Sincere thanks to the reviewers of this particular text. **Note**: The

original text was entirely crafted in Spanish, then corrected and polished by AI. This version was rigorously reviewed and further specifically corrected or adapted by the writer. This final version was translated by AI, which in turn was meticulously reviewed and specifically corrected by the author, as presented in this final versión.

References

- Afanasiev, V., Kovalevsky, V., Yelisseyev, A., Mashkovtsev, R., Gromilov, S., Ugapeva, S., Barabash, E., Ivanova, O. & Pavlushin, A. (2024). About the origin of carbonado. *Minerals*, 14(9): 927. https://doi.org/10.3390/min14090927.
- Afanasiev, V.P., Efimova, E.S., Zinchuk, N.N. & Koptil, V.I. (2000). *Atlas morfologii almazov Rossii*. Novosibirsk: Siberian Branch of the Russian Academy of Sciences Scientific Research Center. 298 pp.
- Akulov, N.I. (2022). Testing of sedimentary deposits at diamond searching works. Melbourne: Aus Publishers. 212 pp.
- Cartigny, P. (2010). Mantle-related carbonados? Geochemical insights from diamonds from the Dachine komatiite (French Guiana). *Earth and Planetary Science Letters*, 296(3–4): 329–339. https://doi.org/10.1016/j.epsl.2010.05.015>.
- Dobrzhinetskaya, L., Faryad, S.W., Wallis, S. & Cuthbert, S. (2012). *Ultrahigh-pressure metamorphism 25 years after the discovery of coesite and diamond*. Amsterdam: Elsevier Insights. 406 pp.
- Erlich, E.I. & Hausel, W.D. (2002). *Diamond deposits: origin, exploration, and history of discovery*. Littleton, CO: Society for Mining, Metallurgy, and Exploration, Inc. 264 pp.
- Fukura, S., Nakagawa, T. & Kagi, H. (2005). High spatial resolution photoluminescence and Raman spectroscopic measurements of a natural polycrystalline diamond, carbonado. *Diamond and Related Materials*, 14(11–12): 1950–1954. https://doi.

- org/10.1016/j.diamond.2005.08.046>.
- Guo, X., Xu, J., Sun, Z., Hui, F., Liang, Y. & Liang, H. (2024). Effect of Al contents on Raman spectra of MgSiO₃ perovskite. *ECS Journal of Solid State Science and Technology*, 13(1): 013001. https://doi.org/10.1149/2162-8777/ad16f7>.
- Haggerty, S.E. (2017). Carbonado diamond: a review of properties and origin. *Gems & Gemology*, 53: 168–179.
- Harris, J.W., Fedortchouk, Y. & Moore, M. (2022). Morphology of monocrystalline diamond and its inclusions. *Reviews in Mineralogy and Geochemistry*, 88: 119–166. https://doi.org/10.2138/rmg.2022.88.02.
- Kaminsky, F.V. (2012). *The Earth's lower mantle: composition and structure*. Cham: Springer. 331 pp. https://doi.org/10.1007/978-3-319-55684-0.
- Ketcham, R.A. & Koeberl, C. (2013). New textural evidence on the origin of carbonado diamond: An example of 3-D petrography using X-ray computed tomography. *Geosphere*, 9(6): 1336–1347. https://doi.org/10.1130/GES00908.1.
- Litvin, Y.A. (2017). *Genesis of diamonds and associated phases*. Cham: Springer. 418 pp.
- Manning, C.E., Lin, J-F. & Mao, W.L. (Eds.). (2020). *Carbon in Earth's interior*. Hoboken, NJ y Washington, D.C.: American Geophysical Union y John Wiley and Sons, Inc. 398 pp.
- Masaitis, V.L. (Ed.). (2019). *Popigai impact structure and its diamond-bearing rocks*. Cham: Springer International Publishing AG. 356 pp. https://doi.org/10.1007/978-3-319-77988-1>.
- Mitchell, R.H. (1986). *Kimberlites: mineralogy, geochemistry, and petrology*. New York: Springer Science+Business Media, LLC. 438 pp. https://doi.org/10.1007/978-1-4899-0568-0>.
- Mitchell, R.H. (1995). *Kimberlites, orangeites, and related rocks*. New York: Springer Science+Business Media, LLC. 456 pp.

- https://doi.org/10.1007/978-1-4615-1993-5.
- Mitchell, R.H. & Bergman, S.C. (1991). *Petrology of lamproites*. New York: Springer Science+Business Media, LLC. 478 pp. https://doi.org/10.1007/978-1-4615-3788-5.
- Németh, P., Garvie, L.A.J. & Salzmann, C.G. (2023). Canyon Diablo lonsdaleite is a nanocomposite containing c/h stacking disordered diamond and diaphite. *Philosophical Transactions of the Royal Society A: Mathematical, Physical and Engineering Sciences*, 381: 20220344. https://doi.org/10.1098/rsta.2022.0344.
- Németh, P., McColl, K., Garvie, L.A.J., Salzmann, C.G. & McMillan, P.F. (2022). Impact-formed complex diamond-graphite nanostructures. *Resolution and Discovery*, 2022: 2051.
- Orcutt, B.N., Daniel, I. & Dasgupta, R. (Eds.). (2020). *Deep carbon: past to present*. Cambridge: Cambridge University Press. 502 pp. https://doi.org/10.1017/9781108677950.
- Petrovsky, V.A., Shiryaev, A.A., Lyutoev, V.P., Sukharev, A.E. & Martins, M. (2010). Morphology and defects of diamond grains in carbonado: clues to carbonado genesis. *European Journal of Mineralogy*, 22(1): 35–47. https://doi.org/10.1127/0935-1221/2010/0022-1978.
- Presser, J.L.B. (2001). *Proyecto Curuguaty, Dpto. de Canindeyú, Paraguay Oriental*. (Trabajo de grado). Asunción: Universidad Nacional. 1 pp.
- Presser, J.L.B. (2019). *Diamonds occurrences* in *Paraguay*. Asunción: 1er Diamond Deposit Exploration Event. 1 pp.
- Presser, J.L.B. (2024a). *The Capiibary "Diamonds": a window to the lower mantle*. Chisinau: Eliva Press. 325 pp.
- Presser, J.L.B. (2024b). Lonsdaleite diamonds in the mantle: as an example of the Capiibary diamonds. *Geology Earth Science En*-

- deavor Research Group, 2024 5th Global Scientific Congress on Geology and Earth Science. Valencia: GESERG. 2 pp.
- Presser, J.L.B. (2025). Lower mantle lonsdaleite. Boletín del Museo Nacional de Historia Natural del Paraguay, 29(e2025004): 1–15.
- Presser, J.L.B., Bulanova, G.P. & Smith, C.B. (2014). Diamantes de Capiibary, Dpto. San Pedro, Paraguay. *Boletín del Museo Nacional de Historia Natural del Paraguay*, 17(2): 5–23.
- Presser, J.L.B., Monteiro, M. & Maldonado, A. (2020). Impact diamonds in an extravagant metal piece found in Paraguay. *Historia Natural*, 10(2): 5–15.
- Presser, J.L.B., Sikder, A. (2022). Raman spectroscopic analysis of diamonds and his mineral inclusions from "lamproites" in the Capiibary, San Pedro Dpto., Paraguay. *Historia Natural*, 3(12)3: 5–19.
- Presser, J.L.B., Sikder, A.M. & Connelly, D.P. (2024c). The Musgrave impact diamonds from MAPCIS very probable impact basin, West Central Australia. *Boletín del Museo Nacional de Historia Natural del Paraguay*, 28(e2024009): 47–57.
- Presser, J.L.B., Sikder, A.M. & Meyer, C. (2024a). Onset XRD analysis of lonsdaleite diamonds from "lamproites" in the Capiibary, San Pedro Dpto, Paraguay. Pp. 234–256, *in* Presser, J.L.B. (Ed.). *The Capiibary "Diamonds": a window to the lower mantle*. Chisinau: Eliva Press. 325 pp.
- Presser, J.L.B., Sikder, A.M. & Meyer, C. (2024b). Lonsdaleite diamonds from "lamproite" in the Capiibary, San Pedro Dpto, Paraguay. Pp. 210–233, *in* Presser, J.L.B. (Ed.). *The Capiibary "Diamonds": a window to the lower mantle*. Chisinau: Eliva Press. 325 pp.
- Presser, J.L.B. & Sikder, A.M. (2024d). Impact diamonds in an extravagant metal piece found in Paraguay: published

- Raman spectra revisited. *Revista de la Sociedad Científica del Paraguay*, 29(1): 22–42. https://doi.org/10.32480/rscp.2024.29.1.22.
- Presser, J.L.B., Tondo O., M.J., Fariña Dolsa, S., Rocca, M.C.L., Alonso, R.N., Benítez, P., Larroza C., F.A., Rodríguez Duarte, B.J. & Cabral-Antúnez, N.D. (2017). Breves comentarios sobre el metamorfismo de impacto en cuarcitas del Cerro León, Paraguay-Occidental. *Pyroclastic Flow*, 7(1): 16–24.
- Simakov, S., Scribano, V., Melnik, N., Pechnikov, V., Drozdova, I., Vyalov, V. & Novikov, M. (2023). Nano and micro diamond formation in nature ultrafine carbon particles on Earth and space. Cham: Springer Nature. 132 pp. https://doi.org/10.1007/978-3-031-43278-1.
- Smith, C.B., Bulanova, G.P. & Presser, J.L.B. (2012). *Diamonds from Capiibary, Paraguay*. 10th International Kimberlite Conference Extended Abstract No. 10IKC-36. 5 pp.
- Smith, E.M. (2021). Raman spectra catalogue for inclusions in diamond. (Base de datos científica). Edmonton: University of Alberta. [Consulted: 8.vii.2025]. https://doi.org/10.7939/DVN/JEHGBW>.

- Smith, E.M., Krebs, M.Y., Genzel, P.T. & Brenker, F.E. (2022). Raman identification of inclusions in diamond. *Reviews in Mineralogy and Geochemistry*, 88(1): 451–473. http://dx.doi.org/10.2138/rmg.2022.88.08>.
- Sorokhtin, N.O. (2019). *The origins of natural diamonds*. Beverly, MA y Hoboken, NJ: Scrivener Publishing y John Wiley & Sons, Inc. 368 pp.
- Stachel, T., Brey, G.P. & Harris, J.W. (2022). Mineral inclusions in lithospheric diamonds. *Reviews in Mineralogy and Geochemistry*, 88(1): 301–394. https://doi.org/10.2138/rmg.2022.88.06>.
- Sung, J. (2021). Handbook of industrial diamonds superabrasives and diamond syntheses, Vol. 1. Singapore: Jenny Stanford Publishing Pte. Ltd. 545 pp.
- Tappert, R. & Tappert, M.C. (2011). *Diamonds in nature: a guide to rough diamonds*. Berlin: Springer-Verlag Berlin Heidelberg. 138 pp.
- Walter, M.J., Thomson, A.R. & Smith, E.M. (2022). Geochemistry of silicate and oxide inclusions in sublithospheric diamonds. Pp. 393–450, *in* Reviews in Mineralogy and Geochemistry, 88. Chantilly, VA: Mineralogical Society of America. 540 pp.

Lower Mantle Ultramafic Association Mineral Inclusion in Capii-6 Lonsdaleite Diamond: A Window into Earth's Depths

Appendices

(Prepared with the assistance of Deepseek Machine Learning)

Technical report: XRD-raman analysis of capii-06 diamond (lower mantle origin)

1. Sample description

Macroscopic features: Colorless with smoky tint (~2 mm), distorted rhombohedron. Inclusions: Black, micrometer-to-nanometer scale.

2. XRD Analysis

Refinement (FullProf):

- PHASE 1 Lonsdaleite (P6₃/mmc)
- CELL 2.508 2.508 4.108 90 90 120
- PHASE 2 Diamond (Fd-3m)
- CELL 3.563 3.563 3.563 90 90 90

Results:

- Lonsdaleite: $87.5\% \pm 0.5\%$, crystallite size = 12 ± 1 nm, strain = 0.15%.
- Diamond: $5.0\% \pm 0.3\%$, crystallite size = 50 ± 5 nm.
- Quality: Rwp = 8.7%, χ^2 = 1.05.

Key peaks:

- 43.72° 2θ (111, lonsdaleite/diamond overlap).
- Triplet peak (43–44° 2θ, lonsdaleite signature).

Band	Center (cm ⁻¹)	FWHM (cm ⁻¹)	Assignment
Lonsdaleite	1332	12	E2g mode (hexagonal)
Diamond	1330	8	F ₂ g mode (cubic)
D-band	1350	30	sp³/sp² defects
G-band	1580	40	Disordered graphite

3. Raman spectroscopy

Peak Decomposition (lmfit):

Spectral Types:

- Type I (68%): FWHM < 5 cm⁻¹ (high crystallinity).
- Type II/III: Broad peaks (FWHM up to 154 cm⁻¹) → nanocrystalline lonsdaleite.

4. Mineral inclusions

Identified Phases:

- 1. Bridgmanite (MgSiO₃):
 - Size: 200–500 nm (retrogressed to enstatite + corundum).
 - Raman: Peaks at 670, 920 cm⁻¹.
- 2. Ferropericlase (Mg,Fe)O:
 - Size: 100–300 nm.
 - Raman: 600-800 cm⁻¹.
- 3. Breyite (CaSiO₃):
 - Size: <100 nm (retrogressed Ca-perovskite).
 - Raman: 1040 cm⁻¹.
- 4. Amorphous SiO₂:
 - Size: Nanoscale (Raman: 695 cm⁻¹, FWHM > 20 cm⁻¹).

5. Formation conditions**

- Pressure: 25–29 GPa (from ferropericlase XRD + Raman FWHM).
- Equation: P(GPa) = (0.3416 * FWHM) + 3.2044 (Table 1).
- Origin: Lower mantle (bridgmanite-ferropericlase association).

6. Conclusions

1. **Hybrid structure:** Dominant lonsdaleite (87.5%) with nanocrystalline diamond (5%) and amorphous phases (7.5%). =94.6% Lonsdaleite and 5.4% Nanocrystalline Diamond.

Interpretation: This ratio describes a near-pure lonsdaleite material with a small fraction of nanocrystalline diamond, likely acting as a grain-boundary filler to enhance toughness and reduce brittleness.

- **2. Inclusions:** Bridgmanite + ferropericlase + breyite confirm lower mantle origin (25–29 GPa).
- **3. Key novelty:** First documented lonsdaleite diamond with ultramafic inclusions.

Diamond Type Classification for Capii-06 (Based on XRD + Raman Data)

Parameter	Type I	Type II	Type III
D-peak (cm ⁻¹)	1331 (narrow)	1331 + G-peak (1580)	1330 + G-peak (1580)
FWHM (cm ⁻¹)	<5 (high crystallinity)	5–20	>20 (up to 154)
Nitrogen Features	None detected	Possible IaA/IaB	Disordered sp ³ /sp ²
% in Capii-06	68%	22%	10%

1. Raman Spectroscopy Classification

Conclusion:

- **Dominant Type I** (68% spectra) → Low nitrogen, high crystallinity.
- **Subtype IaA/IaB** (Type II) suggested by moderate FWHM and G-peak in 22% spectra.
- Type III (10%) indicates nanocrystalline/disordered carbon (lonsdaleite influence).

2. XRD Supporting Evidence

- No nitrogen-related peaks in XRD → Supports Type IIa (nitrogen-free) for cubic diamond component.
- **Lonsdaleite (87.5%)**: Hexagonal carbon lacks nitrogen incorporation → Consistent with Type II behavior.

3. Final Classification

Component	Diamond Type	Rationale
Cubic Diamond	IIa	No nitrogen in XRD; narrow D-peak (Type I Raman).
Lonsdaleite	N/A	Hexagonal carbon; no nitrogen sites.
Disordered Carbon	III	High FWHM, M-shaped peaks (Raman).

Note:

- Anomaly: Inverse intensity-FWHM correlation suggests mixed hybridization (sp³/sp²) due to lonsdaleite-diamond interface.
- **Not Type Ib**: No isolated nitrogen (no 1130 cm⁻¹ Raman peak).